Renewable and Sustainable Energy Reviews 15 (2011) 630–638

Contents lists available at ScienceDirect

Renewable and Sustainable Energy Reviews

journal homepage: www.elsevier.com/locate/rser

Thermal analysis and performance optimization of a solar water heater flat plate collector: Application to Tétouan (Morocco)

Hanane Dagdougui [a,b,*], Ahmed Ouammi [a,c], Michela Robba [a], Roberto Sacile [a]

[a] Department of Communication, Computer and System Sciences (DIST), University of Genova, Italy
[b] MINES ParisTech, CRC-Centre for Research on Risk and Crises, Sophia Antipolis Cedex, France
[c] Energetic Laboratory, Sciences Faculty, Abdelmalek Essaadi University, Tétouan, Morocco

ARTICLE INFO

Article history:
Received 4 August 2010
Accepted 2 September 2010

Keywords:
Optimization
Thermal performance
Solar water heating system
Flat plate solar collector
Decision support systems

ABSTRACT

The development of sustainable energy services like the supply of heating water may face a trade-off with a comfortable quality of life, especially in the winter season where suitable strategies to deliver an effective service are required. This paper investigates the heat transfer process as well as the thermal behavior of a flat plate collector evaluating different cover configurations. This investigation is performed according to a two-folded approach. Firstly, a complete model is formulated and implemented taking into account various modes of heat transfer in the collector. The goal is to investigate the impact of the number and types of covers on the top heat loss and the related thermal performance in order to support decision makers about the most cost-effective design. The proposed model can also be used to investigate the effect of the different parameters which may affect the performance of the collector. Secondly, a two objective constrained optimization model has been formulated and implemented to evaluate the optimality of different design approaches. The goal is to support decision makers in the definition of the optimal water flow and of the optimal collector flat area in order to give a good compromise between the collector efficiency and the output water temperature. The overall methodology has been tested on environmental data (temperature and irradiation) which are characteristic of Tétouan (Morocco).

Contents

1. Introduction . . . 631
2. FPSC heat transfer modeling . . . 632
    2.1. Computational approach . . . 632
    2.2. Reference models . . . 633
        2.2.1. Klein method . . . 633
        2.2.2. Akhtar method . . . 633
3. Optimization of the FPSC design . . . 633
    3.1. FPSC thermal performance . . . 633
    3.2. The optimization problem . . . 634
4. Results and discussions . . . 634
    4.1. Modelling FPSC heat losses . . . 635
    4.2. The optimization results . . . 637
5. Conclusion . . . 638
    References . . . 638

* Corresponding author at: c/o DIST, University of Genova, c/o Savona Campus, via Magliotto 2, 17100 Savona, Italy.
E-mail address: hanane.dagdougui@unige.it (H. Dagdougui).

1364-0321/$ – see front matter © 2010 Elsevier Ltd. All rights reserved.
doi:10.1016/j.rser.2010.09.010

Nomenclature

U_G	global heat loss coefficient (W/m^2 K)
U_B	bottom heat loss coefficient (W/m^2 K)
U_E	edge heat loss coefficient (W/m^2 K)
U_T	top heat loss coefficient (W/m^2 K)
$hr_{i,i+1}$	radiation coefficient between two adjacent layers (W/m^2 K)
$hc_{i,i+1}$	convection coefficient between two adjacent layers (W/m^2 K)
h_{fi}	radiation coefficient between absorber plate and first cover (W/m^2 K)
V	wind speed (m/s)
I	solar radiation (W/m^2)
T_a	ambient temperature (K)
T_p	absorber plate temperature (K)
T_{fi}	water inlet temperature (K)
T_{fo}	water outlet temperature (K)
T_c	cover temperature (K)
$T_{c,i}$	temperature of the ith cover (K)
T_m	average temperature of the enclosed space (K)
T_s	sky temperature (K)
E_i	emissivity of the ith layer (dimensionless)
σ	Stefan–Boltzman constant (W/m^2 K^{-4})
N	number of glass covers (dimensionless)
N_u	Nusselt number (dimensionless)
k	conductivity of the air gap (W/m K)
l	plate cover spacing (m)
Ra	Rayleigh number (dimensionless)
Pr	Prandtl number (dimensionless)
ν	kinematic viscosity of air (m^2 s^{-1})
$\tau\alpha$	optical efficiency of the collector (dimensionless)
τ_c	transmission coefficient of the cover (dimensionless)
α_p	absorptance of the absorber plate (dimensionless)
ρ_c	reflection coefficient (dimensionless)
$h_{N,N+1}$	wind convection coefficient (W/m^2 K)
F'	collector efficiency factor (dimensionless)
C_{pf}	specific heat of water (J/kg K)
$\dot{m}_f$	water mass flow rate (kg/s)
η	collector efficiency (dimensionless)
D	tube diameter (m)
w	width of the absorber area (m)
β	tilt angle (°)
A_c	collector area (m^2)

1. Introduction

Nowadays, renewable energy is considered as the key to a sustainable energy future. It can have a beneficial impact on the environmental, economic, and political issues of the world. Fossil fuel price increase, climate change, adverse environmental impacts – in brief the respect of the Kyoto agreement – makes the exploration for a sustainable way to use energy more important than ever. Soteris [1] has recently shown that the benefits arising from the installation and operation of renewable energy systems can be classified into three categories: energy saving, generation of new working posts, and the decrease of environmental pollution. Solar energy may play an outstanding role to substitute non-renewable energy sources as it may also play an important prerequisite to enhance sustainable development.

Solar water heating systems (SWHS) are very common systems, extensively used in many countries with good solar radiation potential, such as in the Mediterranean countries. SWHS are often viable to replace electricity and fossil fuels used for many home applications [2]. In general in a SWHS, conventional flat plate solar collectors (FPSCs) with a metal absorber plate and covers are used to transform solar energy into heat [3]. In a FPSC, the incident solar radiation is converted into heat and transmitted to a transfer medium such as water.

Several FPSC designs have been proposed and discussed in literature. Different aspects can be investigated comparing the performances of those systems. These aspects can be mainly classified in: the thermal performance, lifetime and cost, sustainability or durability, maintenance and installation devices [4].

FPSC thermal performances can be modelled according to complex functions of the meteorological data, of the design system and finally of the operating conditions. Since the meteorological conditions cannot be modified, the FPSC performance can be enhanced working either on the operations conditions or on the SWHS components. In the design of SWHS components, care should be especially given to the number and nature of the transparent covers and on the selectivity of the absorber [5]. Glass is a quite common choice as a cover for solar thermal devices since it absorbs almost all the infrared radiation (IR) re-emitted by the absorber plate, and then leads to a reduction of the greenhouse effect which is responsible of the enhancement of the thermal efficiency of the solar collector. On the other hand, the use of a glass cover in rural zones of developing countries has two major disadvantages: its high installation cost, and its fragility both during transportation and in service [6]. So, some authors [7,8] recommend the use of plastic covers because of their relatively low weight and good resistance against shocks. On the other hand, the long-term plastic cover exposition leads to degradation.

Although theoretical simplified approaches have been available for many decades, an exhaustive FPSC thermal analysis is still a hard task since several characterizing parameters are required. In literature, there are numerous studies on the SWHS performance analysis.

Akhtar and Mullick [9] proposed a model to compute the FPSC glass cover temperature with single glazing, and then [10] enhanced this model proposing a set of relations to compute the glass cover temperatures for double glazing. The values of top heat loss coefficient are computed and are close to the numerical solutions of heat balance equations.

Smyth et al. [11] discussed integrated collector storage solar water heaters. Kaldellis et al. [12] presented an analysis of the time variation of the local market taking seriously into account the domestic solar water heating system annual replacement rate. Batidzirai et al. [13] demonstrated the importance and significance of water heating in the national energy end-use regime in Zimbabwe and concluded that solar water heating can result in economic, social and environmental benefits for the whole country. It shows that water heating in the residential, health and tourism sectors contributes about 13% of the coincident winter peak demand and accounts for 8% of final electricity consumed in the country. Muneer et al. [14] investigate the possibility of exploitation of solar energy within the Turkish textile industry with particular reference to thermal application and presented a detailed life cycle assessment and relevant economics of solar water heater. Muneer et al. [15] proposed an introduction of built-in-storage water heaters for Pakistani textile industry. They presented a comparison of the thermal performance of two

different designs of built-in storage water heater plain and newly designed finned type. Armando and Oliveira [16] presented a new approach to express the long-term performance of general solar thermal systems. Jannot and Coulibaly [6] presented a new set of equations for the radiative balances of the absorber plate and the transparent cover of a solar air heater covered with a plastic film. Janjai et al. [3] developed a mathematical model to simulate the performance of a large area plastic solar collector. Bilgen and Bakeka [17] designed and studied a simple solar system and evaluated its economics and thermal performance. Soteris [1] studied the thermal performance, economics and environmental protection offered by thermosiphon solar water heating system and showed that a considerable percentage of the hot water needs of the family can be satisfied by solar energy.

The general aim of this work is to support decision makers in the FPSC design phase and in the control of the inlet water flow in the FPSC in order to optimize the FPSC efficiency. This aim is achieved according to a two-folded approach. Firstly, as described in Section 2, a model is formulated and implemented taking into account various modes of heat transfer in the collector. The goal is to investigate the impact of the number and of the types of the covers on the top heat loss and the related thermal performance in order to support decision makers about the most cost-effective design. The proposed model can also be used to investigate the effect of the different parameters which may affect the performance of the collector. Secondly, as described in Section 3, a two objective constrained optimization problem has been formulated and implemented to evaluate the optimality of the performance of different design approaches. The goal is to support decision makers in the definition of design parameters, i.e., the absorber plate area, the pipes' diameter, the mass flow rate, and distance between the tubes. Section 4 shows an application of the proposed methodology with environmental temperature and irradiation characteristics of Tétouan (Morocco). Conclusions and future research directions are finally shown.

2. FPSC heat transfer modeling

The evaluation of the thermal loss coefficients is the fundamental task to assess the FPSC performance.

The FPSC global heat loss coefficient U_G (W/m^2 K) is the sum of the top loss (U_T), the bottom (U_B), and the edges (U_E) coefficients. This loss value is established between the collector and its surrounding by conduction, infrared solar radiation and convection [18]:

$$U_G = U_T + U_B + U_E \tag{1}$$

According to Ref. [19], in an efficient design, the edge and the bottom loss coefficients are smaller than the top heat loss coefficient. In addition, assuming that the FPSC insulation of the edges and of the bottom is responsible for the resistance to heat flow, the sum of the edge and bottom heat loss coefficients can be set to a constant value A.

$$U_G = U_T + A \tag{2}$$

In this paper, the top heat loss coefficient is referred to a FPSC model with N covers. Specifically, the heat loss is referred to several FPSC layers, identified by the index i, $i = 0,\ldots,N + 1$, where the index 0 is referred to the plate adsorber p, $i = 1$ is referred to the bottom cover, $i = 2$ is referred to the second cover (if present), $i = N$ is the top cover, and $N + 1$ is the external environment or ambient a.

The overall energy loss coefficient through the top, U_T, can be assumed as the result of convection and radiation heat losses between parallel plates (or layers). That is:

$$U_T = \left(\sum_{i=1}^{N-1}\left(hc_{i,i+1} + hr_{i,i+1}\right)^{-1}\right)^{-1} \quad i = 0,\ldots,N-1 \tag{3}$$

The radiation coefficients $hr_{i,i+1}$ (W/m^2 K) are expressed by Ref. [3]:

$$hr_{i,i+1} = \frac{\sigma(T_i + T_{i+1})(T_i^2 + T_{i+1}^2)}{(1/E_i) + (1/E_{i+1}) - 1} \quad i = 0,\ldots N-1 \tag{4}$$

$$hr_{N,N+1} = \frac{\sigma E_N(T_N^4 - T_s^4)}{T_N - T_a} \tag{4bis}$$

where $hr_{N,N+1}$ represents the radiation exchange between the outer cover and the sky, E_N (dimensionless) is the emissivity of the Nth cover, T_N (K) is the temperature of the Nth cover (cover with direct contact with the ambiance), T_a represents the ambient temperature (K) and T_s is the considered to be the sky temperature (K).

The convection heat loss coefficients $hc_{i,i+1}$ (W/m^2 K) are conducted through the free convection heat transfer existing in the incarcerate air between the adjacent surfaces. Eq. (5) defines the $hc_{i,i+1}$ coefficient between the absorber and the first inner cover, as well as between two adjacent covers [5], as a function of $k_{i,i+1}$ (W/m K), the conductivity of the air between the layer i and $i+1$, and the distance $l_{i,i+1}$ (m) between the layer i and $i+1$. Eq. (5bis) empirically defines the outer convection loss coefficient in term of the wind velocity V (m/s).

$$hc_{i,i+1} = \frac{k_{i,i+1} Nu_{i,i+1}}{l_{i,i+1}} \quad i = 0,\ldots,N-1 \tag{5}$$

$$h_{N,N+1} = 2.8 + 3V \tag{5bis}$$

Regarding the experimental investigations in the literature [20], the relationship between the Nusselt number and Rayleigh number for tilt angles of the FPSC from 0° to 75° is:

$$\begin{aligned} Nu_{i,i+1} = {} & 1 \\ & + 1.44\left[1 - \frac{1708(\sin\ 1.8\beta)^{1.6}}{Ra_{i,i+1}\ \cos\ \beta}\right]\left[1 - \frac{1708}{Ra_{i,i+1}\ \cos\ \beta}\right]^{+} \\ & + \left[\left(\frac{Ra_{i,i+1}\ \cos\ \beta}{5830}\right)^{1/3} - 1\right]^{+} \quad i = 0,\ldots,N-1 \end{aligned} \tag{6}$$

where the apex (+) is referred to the condition that only positive values of the terms in the square brackets are used.

The Rayleigh number Ra_i (dimensionless) is given by Ref. [20]:

$$Ra_{i,i+1} = \frac{gPr_{i,i+1}(T_i - T_{i+1})l_{i,i+1}^3}{T_m \cdot \nu_{i,i+1}^2} \quad i = 0,\ldots,N-1 \tag{7}$$

where for $i = 0$, $T_0 = T_P$, and $Pr_{i,i+1}$ (dimensionless) is the Prandtl number at the air gap between the layer i and $i+1$ which depends on the average temperature $T_{mi,i+1} = (T_i + T_{i+1} + 1)/2$; g (m s^{-2}) the gravitational acceleration, and $\nu_{i,i+1}$ (m^2 s^{-1}) is the cinematic viscosity at the air gap between the layer i and $i+1$.

2.1. Computational approach

The top heat loss may be computed according to several empirical relations. Hereinafter, an algorithm is proposed to compute it, on the basis of the direct computation of each cover temperature. Considering a steady state energy transfer, the energy exchange from one gap air to the other is equal to the overall energy

exchange between the absorber and the ambient. Under this hypothesis, the following system of equations can be defined:

$$\begin{cases} T_1 = T_p - \dfrac{U_T(T_p - T_a)}{(hc_{p,1} + hr_{p,1})} \\ T_2 = T_1 + \dfrac{(hr_{p,1} + hc_{p,1})(T_p - T_1)}{hc_{1,2} + hr_{1,2}} \\ T_i = T_{i-1} + \dfrac{(hr_{i-2,i-1} + hc_{i-2,i-1})(T_{i-2} - T_{i-1})}{hc_{i-1,i} + hr_{i-1,i}} \\ \vdots \\ \vdots \\ T_N = T_{N-1} + \dfrac{(hr_{,N-1} + hc)(T_{N-2} - T_{N-1})}{hc_{N-1,N} + hr_{N-1,N}} \end{cases} \tag{8}$$

In the case of one cover, taking into account the first equation of the system of Eqs. (8), the equation defined by Eq. (3), and two unknown variables U_T and T_1, a solution can be found in an iterative two-step approach as described below.

In the first step of the first iteration ($i = 1$), the ambient temperature T_a and the temperature of the plate T_p are known. In addition, an hypothesis on the temperature of the first cover, T^1, is made, where the index 1 is referred to the cover and the apex 1 is referred to the iteration. Specifically, T^1 is supposed to vary in a range $T^1 \in [T_a, T_p]$, for example taking into account an average value $T_1^1 = (T_a + T_p)/2$. From Eq. (3), it is possible to compute $\tilde{U}_T$.

In the second step, the current value of $\tilde{U}_T$, as well as the T_a and T_p values, are given as input to the first equation of (8), and a new $\tilde{T}_1^1$ is obtained.

A convergence test is so evaluated. If $\left|T_1^1 - \tilde{T}_1^1\right| < \varepsilon$, where ε is a suitable small value such as $\varepsilon = 10^{-3}$, the algorithm ends. Otherwise a new iteration $i = 2$ is made. In this new iteration, $T_1^2 = \tilde{T}_1^1$. This process will be iterated until the convergence test is satisfied.

If other covers are presents, their temperature can be computed using the same process used for the case of one cover.

2.2. Reference models

In the case study, the results given by the model described above are compared with the results given by two different methods, Chaudhuri [21] and Akhtar and Mullick [9,10]. These methods allow the computation of the top FPSC heat loss coefficient. A description of these methods is briefly quoted hereinafter.

2.2.1. Klein method

The top loss coefficient U_T can be computed using a conventional empirical equation proposed by Ref. [21], and which is:

$$U_T = \left[\frac{N}{(349/T_p)[T_p - T_a/N + \phi]^{0.33}} + \frac{1}{h_{N,N+1}}\right]^{-1} + \frac{\sigma\left(T_p^2 + T_a^2\right)(T_p - T_a)}{(E_p + 0.05N(1 - E_p))^{-1} + [(2N + \phi - 1)/E_g] - N} \tag{9}$$

where $\phi = \left(1 - 0.04h_{N,N+1} + 0.005h_{N,N+1}^2\right)(1 + 0.091N)$, N is the number of glass covers, E_p (dimensionless) is the emittance of the plate, and E_g (dimensionless) is the emittance of glass.

2.2.2. Akhtar method

In the Klein empirical relation, the global top heat loss is evaluated since the cover temperature is unidentified. Thus, the condensed regrouping parameters in the Klein relationship are deficient in the determination of the radiation and convection heat losses coefficients. For these reasons, and to make our approach more consistent, the approximation method of Akhtar and Mullick [9,10] is more appropriate to compare the obtained results. Actually, this method aims to provide an empirical relation for the glass cover temperature T_c while bearing in mind the heat transfer processes in the FPSC. A more detailed description of the method can be found in Akhtar and Mullick [9,10].

3. Optimization of the FPSC design

3.1. FPSC thermal performance

The solar energy, intercepted by the plate absorber is equal to the incident solar radiation reduced by optical losses, which is a function of the optical efficiency. The FPSC optical efficiency strongly depends on the used material type, such as transparent covers. The cover characteristics influence the energy transferred to the absorber, and consequently the thermal performance of the overall system. So, the selection of a suitable component constitutes a fundamental task. The optical efficiency or the effective product transmittance–absorptance is expressed by Ref. [5]:

$$(\tau\alpha) = \frac{\tau_c \alpha_p}{1 - (1 - \alpha_p)\rho_c} \tag{10}$$

where $(\tau\alpha)$ is the FPSC optical efficiency (dimensionless), τ_c is the cover transmission coefficient (dimensionless), α_p is the absorber plate absorptance (dimensionless), and ρ_c is the reflection coefficient (dimensionless).The FPSC performance is described by an energy balance that converts the incident solar energy into useful energy gain, thermal losses and optical losses. Assuming a steady state, the energy balance of different components is expressed by:

$$\dot{m}_f c_{pf} \frac{dT_{fo}}{dx} = F'\ell[(\tau\alpha)I - U_G(T_f - T_a)] \tag{11}$$

with

$$F' = \frac{1/U_G}{w[(1/U_G[D + (w - D)F]) + (1/\pi D h_{fi})]} \tag{12}$$

where $\dot{m}_f$ (kg/s) is the water flow in the FPSC tube, T_{fo} is the outlet water temperature (K), c_{pf} (J/kg K) is the specific heat of water, F' (dimensionless) expresses the FPSC efficiency factor, D (m) is the water tube diameter, w (m) is the width between two centres of adjacent tubes, h_{fi} (W/m^2 K) is the radiation coefficient between absorber plate and first cover and F is the standard fin efficiency (dimensionless) that depends on D, w and $\dot{m}_f$.

Assuming that F' and U_G are independent from the x position (that is referred to the length of the water tube), the solution of (11) is:

$$\frac{T_{fo} - T_a - (\tau\alpha)I/U_G}{T_{fi} - T_a - (\tau\alpha)I/U_G} = \exp(-U_L F' A_c/\dot{m}_f c_{pf}) \tag{13}$$

where T_{fi} is the inlet water temperature and A_c (m^2) is the area of the FPSC.

In the computations quoted hereinafter, the sum of the bottom and the edges losses coefficient A is supposed to be constant and equal to 1.2 W/m^2 K. A measure of the instantaneous FPSC performance is the collector effectiveness, expressed as the ratio of the instantaneous useful thermal power extracted from the water collector $Q_u(t)$ (J) to the instantaneous incident solar irradiation $A_c I(t)$ (J), and it is defined as reported by Farahat et al. [22]:

$$\eta(t) = \frac{Q_u(t)}{A_c I(t)} \tag{14}$$

The evaluation of the daily FPSC efficiency takes place by integrating the previous equations over all the operating solar system hours. This expression could be obtained by integrating from the instant t_r of sunrise to the instant t_s of sunset.

The overall thermal efficiency η during the daytime is calculated from the relationship:

$$\eta = \frac{\int_{t_r}^{t_s} \dot{m}_f c_{pf}(T_{fo} - T_{fi})dt}{A_c \int_{t_r}^{t_s} I(t)dt} \tag{15}$$

where

$$Q_u(t) = \int_{t_r}^{t_s} \dot{m}_f c_{pf}(T_{fo} - T_{fi})dt \tag{15bis}$$

3.2. The optimization problem

The model described in Section 2 highlights the importance of choosing proper design parameters, such as the sizes of the absorber plate, the pipes' diameter, etc., for the performance of the heating through a FPSC. In this section, an optimization approach is followed in order to ensure an optimal performance of the FPSC design. Specifically, the optimization model defined hereinafter aims to find the optimal design of the solar system that offers a maximum efficiency and a maximum outlet water temperature. So, the problem is formalized as a two-objective decision problem, and its application may be useful for decision makers, as it gives the opportunity to obtain the optimal value of several important design options. Moreover, the Pareto optimal solutions, as shown in the case study, may be useful for decision makers since it is possible to identify all the possible scenarios, and, depending on the available financial resources, either a specific solar collector area or a particular working fluid mass flow can be chosen.

In the proposed optimization problem, the decisional variables are related to the main design parameters, i.e., the absorber plate area A_c (m^2), the pipes' diameter D (m), the mass flow rate $\dot{m}_f$ (kg/s), and distance between the tubes of the FPSC, w (m). Two non-commensurable objectives have to be maximized: the outlet temperature of the water, T_{fo} (K), and the efficiency of the overall collector, η (dimensionless).

In a discretized time, the overall objective function is given by the weighted sum of the two contributions. That is:

$$Z = \sum_{t=t_r}^{t_s} T_{fo}^t + \alpha\eta \tag{16}$$

where α (K) is a weighting factor and the optimization instants t are given in hours.

Based on the continuous formulation of Eq. (13), the outlet temperature of the water is given by:

$$T_{fo}^t(A_C, w, D, \dot{m}_f) = \left[T_a^t + \frac{(\tau\alpha)I^t}{U_G} + \frac{T_{fi} - T_a^t - (\tau\alpha)I^t}{U_G} \times \exp\frac{-U_G F' A_c}{\dot{m}_f c_{pf}}\right] \quad t = 1, \ldots, T \tag{17}$$

where the apex t is the time instant, at which ambient temperature and irradiance measurements are also available.

Based on the continuous formulation in Eq. (15), the overall efficiency is:

$$\eta = \frac{\sum_{t_r=1}^{t_s=T} \dot{m}_f c_{pf}\left(T_{fo}^t(A_C, w, D, \dot{m}_f) - T_{fi}\right)}{A_c \sum_{t_r=1}^{t_s=13} I^t} \tag{18}$$

where $t = 1$ is the time of sunrise and $t = T$ is the sunset time.

Different constraints have been taken into account in the optimization problem and are related to the size that may assume the different decision variables. Specifically, there are constraints that limit the size of the diameter, the area, and the distance among tubes to a range of minimum and maximum values. That is:

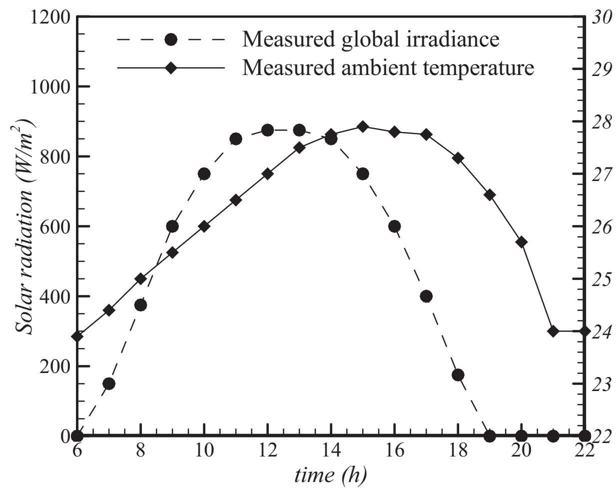

Fig. 1. Climate data used in the simulations.

$$\begin{aligned} D_{min} &\le D \le D_{max} \\ w_{min} &\le w \le w_{max} \\ A_{min} &\le A_c \le A_{max} \end{aligned} \tag{19}$$

where D_{min}, D_{max}, w_{min}, w_{max}, A_{min}, A_{max} are known parameters.

Finally, there are constraints related to the operating parameters that require the existence of maximum and minimum values for the flow rate of the fluid mass. That is:

$$M_{min} \le \dot{m}_f \le M_{max}$$

where M_{min} and M_{max} are known parameters.

4. Results and discussions

Climatic data that are used in the current investigation correspond to the case of a clear type day of July, measured in Tetouan (35°35′N 5°23′W), Morocco [23]. The hourly diffuse radiation has been calculated from the hourly global radiation, using a relation available in the literature [23]. The climatic data are reported in Fig. 1.

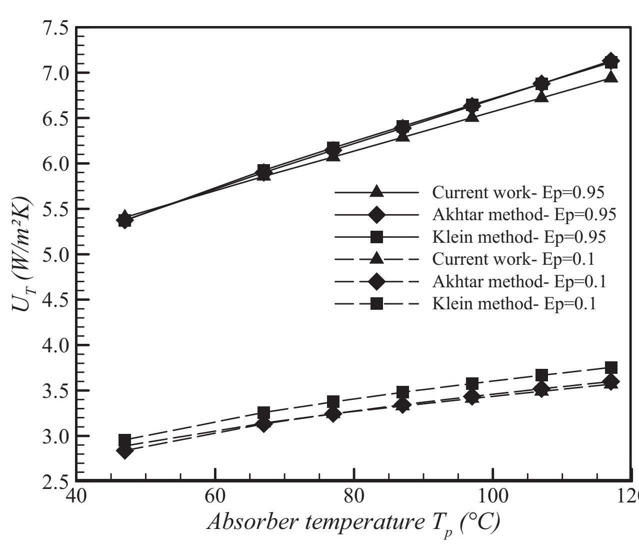

Fig. 2. Top heat loss coefficient versus the absorber plate temperature for one Plexiglas cover.

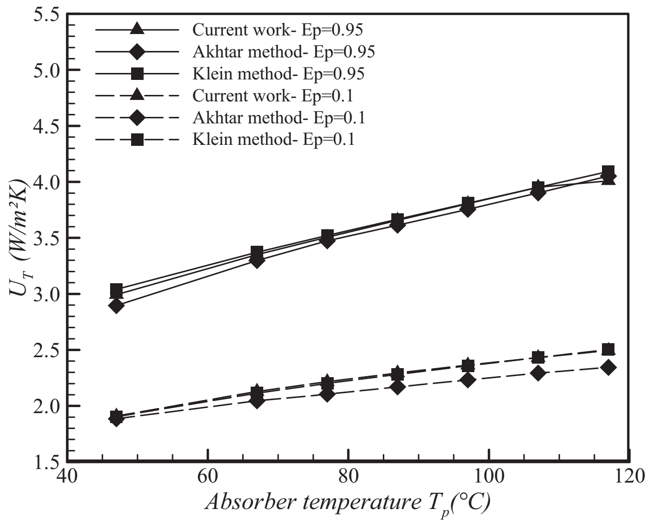

Fig. 3. Top heat loss coefficient versus the absorber temperature for double Plexiglas covers.

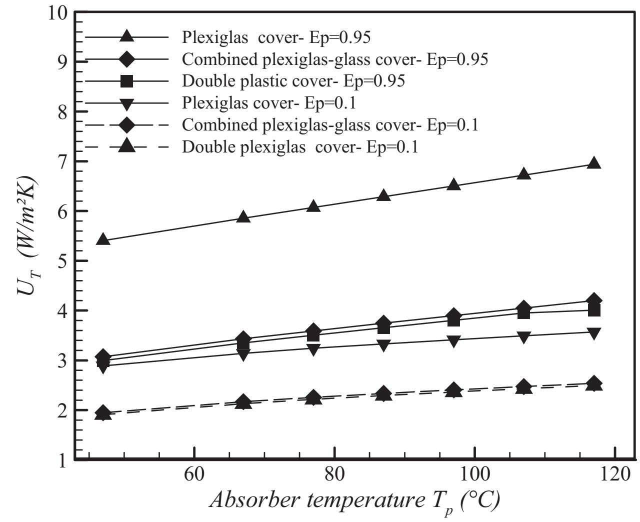

Fig. 5. Top heat loss coefficient versus the plaque absorber temperature for one, and two covers (glass/Plexiglas and Plexiglas/Plexiglas).

4.1. Modelling FPSC heat losses

The top heat loss coefficient U_T is calculated for the FPSC using the iterative numerical method, which seems to be among the most accurate one. A value of 10^{-3} was considered as a residual between two consecutive values of cover temperatures. In order to assess the validity of the proposed method to predict the top heat loss coefficient, the results are compared with some of those existing in the literature. Simulations were first performed for a single cover, at given values of the absorber emissivity, 0.1 and 0.95, which are considered respectively as minimum and maximum values. In Fig. 2, a good agreement was observed between our results and those given by Akhtar and Klein methods. Figs. 3 and 4 display the top heat loss coefficient versus the absorber temperature, for double covers; thus respectively for a double Plexiglas covers, and combined glass Plexiglas covers.

In order to evaluate the performance of the FPSC, Fig. 5 displays the top heat loss coefficient as a function of the absorber temperature, for the three test cases. The heat losses are diminished for a selective plate absorber ($E_p = 0.1$), this kind of cover re-emits a small part of the solar incident irradiation. It can be also remarked that for a selective absorber, either for double Plexiglas covers or combined glass Plexiglas covers, the top heat loss coefficient is approximately equal. However, for a non-selective absorber, double plastic covers were those that give us a slightly higher heat top losses coefficients.

Hence, the combined plastic–glass covers were thus judged to be the most suitable ones in terms of reducing the top heat loss coefficient. Fig. 6 displays the comparison between the ratio of the top heat loss coefficient and the top heat loss at 45°, as a function of a given tilt angle of the collector system. In this latter illustration, results are presented in terms of a normalized value of the heat loss similar to those given by Ref. [19]. It appears that the current results are similar to those presented by Akhtar and Mullick [9,10], and this for both values of emissivities.

The FPSC performance depends on different design components. This study focuses on an assessment of the effect of the absorber emissivity on the heat transfer process. Fig. 7 displays the heat loss coefficient as a function of the emissivity, and that for different type and number of covers. It can be recognized that, whatever the emissivity value, a single Plexiglas cover was the one that gives a higher value of U_T. Similar results are found for double covers (glass/Plexiglas and Plexiglas/Plexiglas). Similar trends are observed between the two kind of double covers.

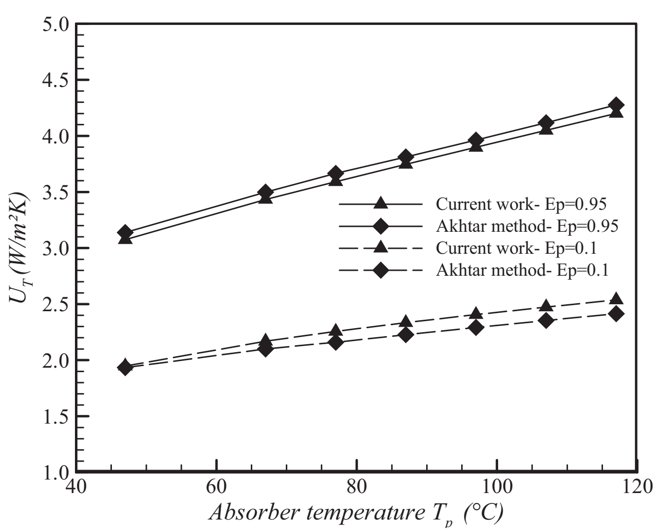

Fig. 4. Top heat loss coefficient versus the absorber temperature for combining glass–Plexiglas covers.

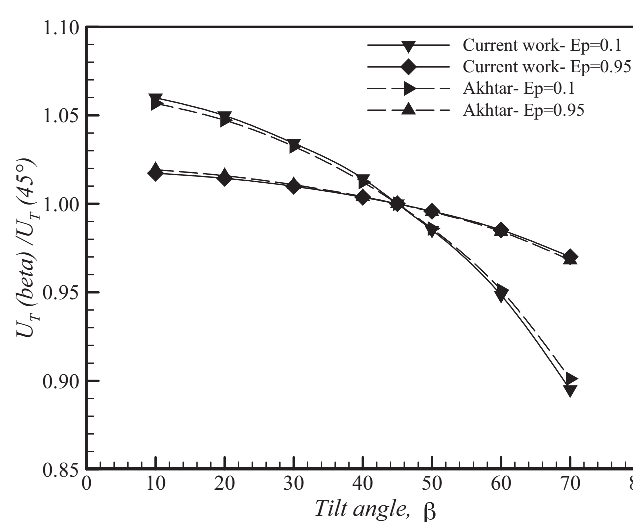

Fig. 6. Ratio of the top heat loss coefficient and the top heat loss coefficient corresponding to 45° as a function of the tilt angle.

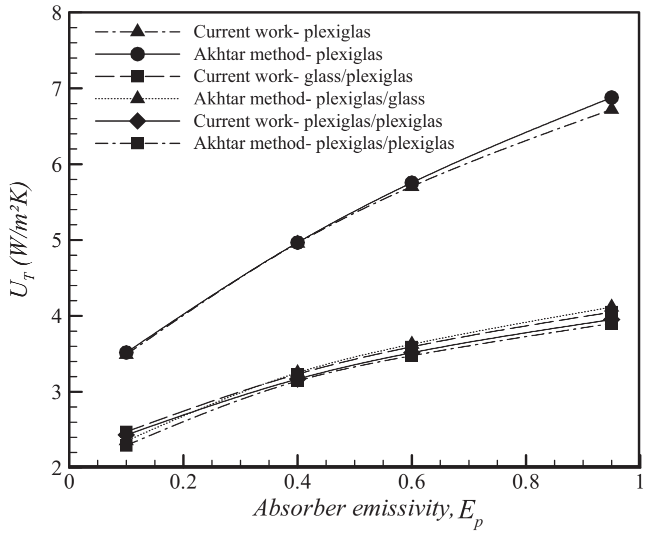

Fig. 7. Top heat loss coefficient against the emissivity of the absorber for single and double covers.

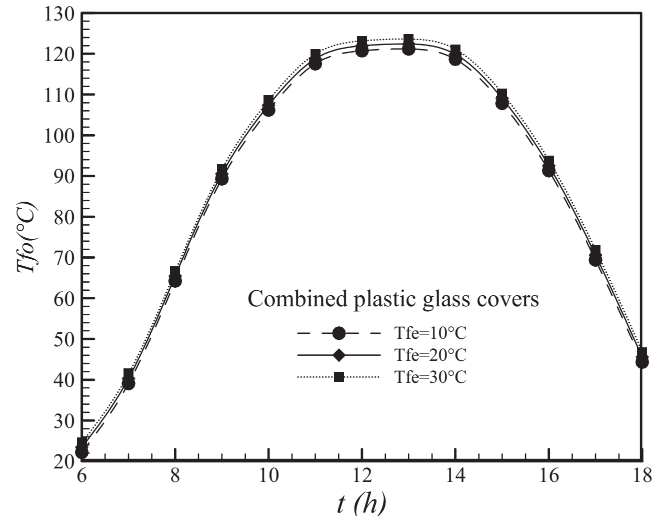

Fig. 9. The effect of inlet water temperature on the hourly variations of the outlet temperature for a combined Plexiglas glass cover.

As a second part, investigations were done on the effects of the variation of the FPSC operation conditions. These investigations included the effects of changing the operation inlet water temperature at a fixed value of flow rate, and, then, the rate at which the water flows in the tubes at a given value of the inlet flow temperature.

Studies were carried out by using two kind of double covers: the double plastic and the combined glass plastic covers. As displayed in Fig. 8, practically, there is no significant difference between the maximum outlet temperature reached by the flat plate for the three values of the inlet temperature, and thus Fig. 9 shows the same trend for the combined covers.

In order to give more details on the performance of both types of covers, Fig. 10 shows the outlet collector temperature at a given value of water flow rate ($\dot{m}_f = 0.001$ kg/s) and at given value of inlet fluid temperature (T_{fi} = 20°). It appears that the combined covers provide a better outlet performance than the double plastic covers. A difference of 7° is observed.

In general, the mass flow rate of the working fluid is one of the most important parameters affecting the performance of solar collectors. In this study, the influence of the mass flow rate on the water outlet temperature and the efficiency was studied. Fig. 11

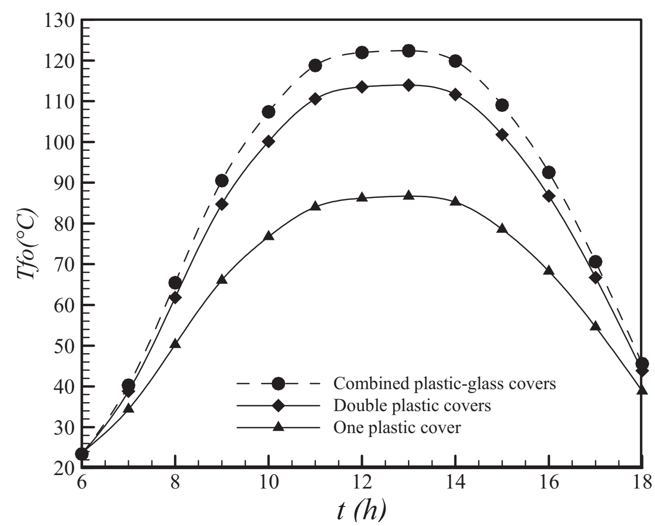

Fig. 10. Comparison of the hourly outlet water temperature for one, combined glass Plexiglas cover and double Plexiglas cover for T_{fi} = 20° and m = 0.001 kg/s.

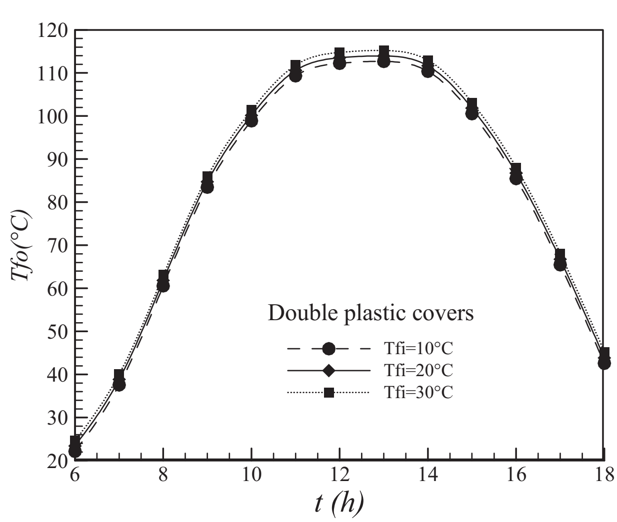

Fig. 8. The effect of inlet water temperature on the hourly variations of the outlet temperature for a double Plexiglas cover.

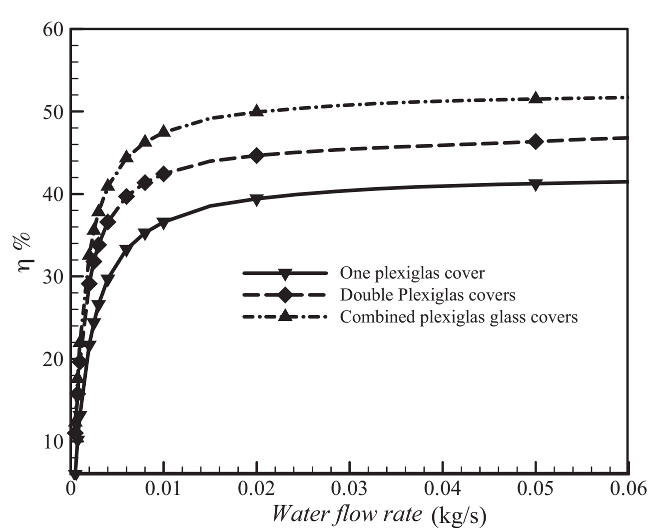

Fig. 11. Efficiency of the FPSC for different kinds of covers.

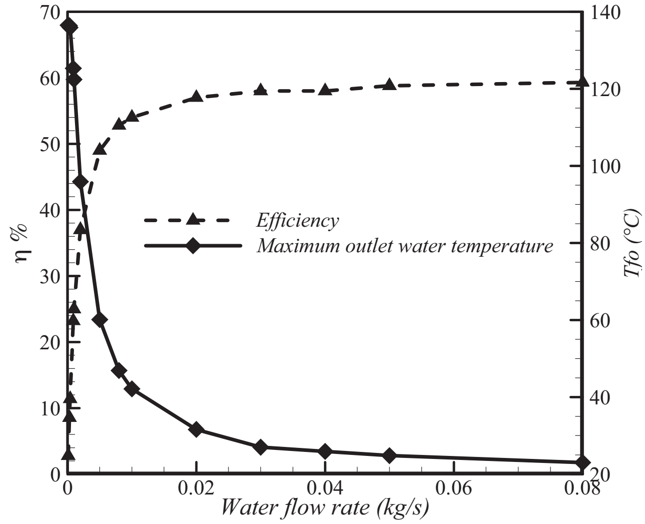

Fig. 12. Maximum outlet water temperature and efficiency of the FPSC versus the water flow rate.

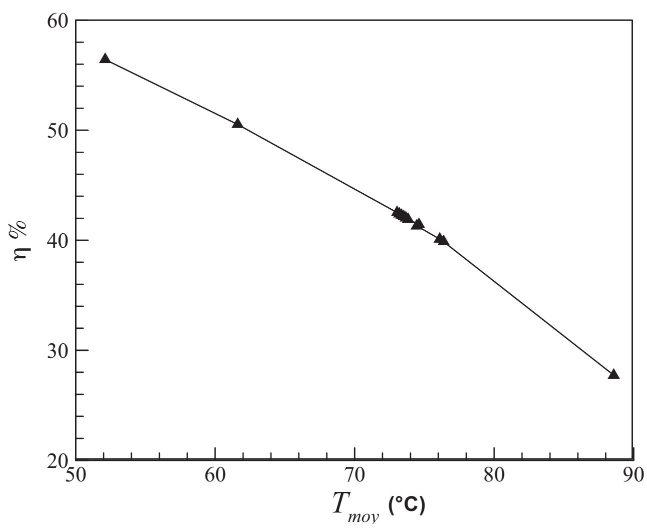

Fig. 13. The collector efficiency versus the output average temperature of water.

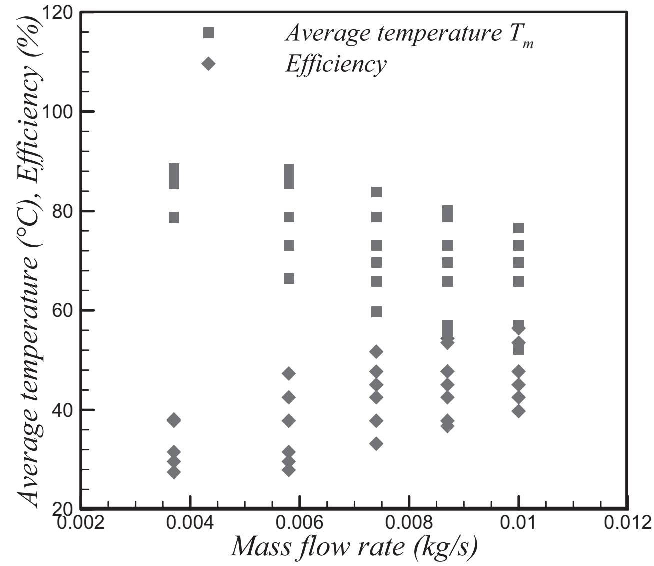

Fig. 14. The variation of collector efficiency and the daily average temperature of water as function of water flow rate.

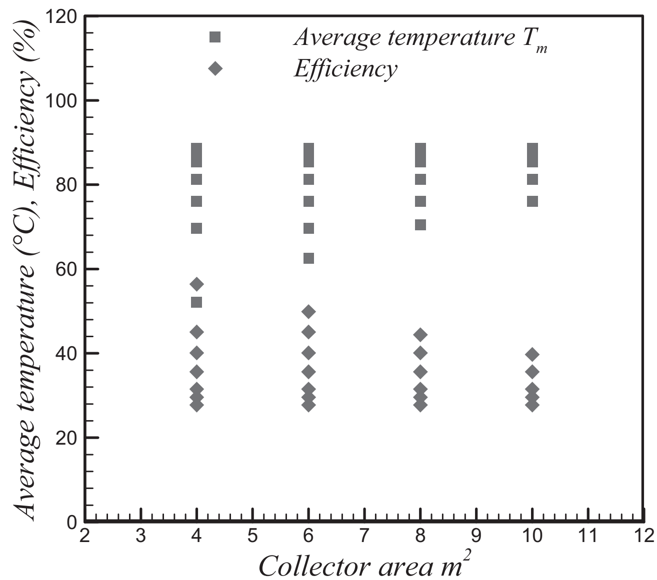

Fig. 15. The variation of collector efficiency and the daily average temperature of water as function of collector area.

shows the effect of the water flow rate on the FPSC daily efficiency, for a single Plexiglas cover, double Plexiglas covers and combined glass Plexiglas covers. This comparison reveals that the glass–Plexiglas covers have much better behavior than the others one. This is especially due to the fact of combining the performances of glass, which has a better transparency to the incident irradiation and the Plexiglas devices that are good for collecting the greenhouse effect. The results in Fig. 12 show that the maximum peak of outlet temperature increases with the decrease of flow rate, while an opposite trend is observed for the effect on the collector efficiency. A value of 2.66×10^{-3} kg/s is considered to be suitable flow rate to maintain good efficiency and adequate fluid outlet temperature.

4.2. The optimization results

The necessary parameters to solve the optimization problem are reported in Table 1. In particular, the non-zero values of solar irradiation and outside temperature are reported. Instead, in Table 2, the non-time dependent parameters are reported.

The optimization problem is non-linear with continuous decision variables. It has been solved for a time horizon of 24 h using the optimization package Lingo 9.0 (www.lindosystems.org). It takes less than 1 min to obtain the optimal local solution.[1]

Fig. 13 shows the results obtained from the optimization process as regards the behavior of the two terms of the objective function, i.e., the efficiency versus the mean outlet temperature. The evolution of the solutions as regards the water flow rate and the collector area according to the objective function are reported respectively in Figs. 14 and 15. Fig. 14 shows the variation of the average outlet water temperature and the collector efficiency according to different values of the weighting factor, thus fixing the value of the mass flow rate (at 0.0037, 0.0058, 0.0074, 0.0087 and 0.01 kg/s). According to this figure, the trend of curve goes by convergence, in others words, the gap between the two set of temperature and the efficiency diminishes as the value of the mass

[1] The multistart optimisation option has been chosen to enhance the reliability of the local optimal solution that have been obtained.

Table 1
Irradiance and ambient temperature of a clear type day of July in Tetouan.

Time (h)	6	7	8	9	10	11	12	13	14	15	16	17	18	19
T_a^t	23.9	24.4	25	25.5	26	26.5	27	27.5	27.75	27.9	27.8	27.5	27.3	26.6
I^t	0	150	375	600	750	850	875	875	850	750	600	400	175	0

Table 2
Inputs data for optimization.

$D_{min} = 0.01$ m	$D_{max} = 0.05$ m
$W_{min} = 0.09$ m	$W_{max} = 0.2$ m
$A_{min} = 1$ m^2	$A_{max} = 10$ m^2
$M_{min} = 0.001$ m^3/s	$M_{max} = 0.008$ m^3/s
$h_{fi} = 300$ W/m^2 K	$m = 5$
$(\tau\alpha) = 0.614$	$T_{fi} = 20^\circ$
$c_{pf} = 4190$	$U_G = 5.31695$ W/m^2 K

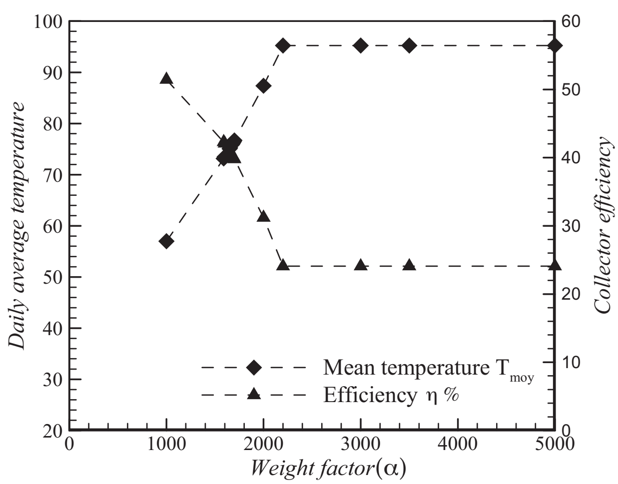

Fig. 16. The effect of the weight factor on collector efficiency and daily average temperature of water.

flow rate increases. Whereas, in Fig. 15, which shows the variation of the average outlet water temperature and the collector efficiency according to different values of the weighting factor, and fixing the values of the collector area at (4, 6, 8 and 10 m^2). In this figure, a divergence of the gap between the average outlet water temperature and the collector efficiency is remarked. The results shown in these two figures are particularly helpful for the selection of the optimal FPSC design. The trends detect the behavior of the collector efficiency and they are associated to the daily average temperature and different decisional variables. Thus, the decision makers, according to their funds and the collector performance requirements, will select the suitable collector area and the operating water flow rate. They will envisage all the possible scenarios, and also choose among a variety of system designs. Fig. 16 shows the variation of the optimal objective function when varying the weighting factor. It can be seen that the efficiency increases with the weighting factor until a critical value of $\alpha = 2198$ K, after which the efficiency does not vary and it is equal to 52.11%. The mean temperature decreases until the same critical value of 2198, and then remains constant at 56.42 °C.

5. Conclusion

In this paper, investigations of the thermal behavior of the FPSC have been done. The goal is to compare the overall loss coefficient of the collector under different numbers and kinds of class covers. The results depicts that the top heat loss (U_T) is lower when adding another cover to the FPSC, it was found that combining plexigals and glass covers gives a better performance to the FPSC. Results of the developed model have been compared with other ones available in the literature, and similar results have been found. Finally, a two-objective non-linear optimization problem has been formalized and solved though mathematical programming technique. Moreover, the optimization problem has been run for different values of the weighting factor (that represents the relative importance given to the two objectives) in order to build the Pareto optimal solutions. The aim of this approach is to find different configurations of the system in order to help decisions makers to choose among a variety of design and system operations. The results show that the water mass flow rate significantly influences the values of the two terms of the objective function, whereas, the effect of the collector area does not have a considerable effect on finding a better compromise between the two conflicting objectives.

References

[1] Soteris A, Kalogirou. Thermal performance, economic and environmental life cycle analysis of thermosiphon solar water heaters. Sol Energy 2009;83:39–48.
[2] Pillai IR, Banerjee R. Methodology for estimation of potential for solar water heating in a target area. Sol Energy 2007;81:162–72.
[3] Janjai S, Esper A, Muhlbauer W. Modelling the performance of a large area plastic solar collector. Renew Energy 2000;21:363–76.
[4] Réné T. A review of the mathematical models for predicting solar air heaters systems. Renew Sust Energy Rev 2009;13:1734–59.
[5] Njomo D, Daguenet M. Sensitivity analysis of thermal performances of flat plate solar air heaters. Heat Mass Transfer 2006;42:1065–81.
[6] Jannot Y, Coulibaly Y. Radiative heat transfer in a solar air heater covered with a plastic film. Sol Energy 1997;60:35–40.
[7] Whiller A. Plastic covers for solar collectors. Sol Energy 1963;3:148–51.
[8] Wijeysundera NE, Iqbal M. Effect of plastic cover thickness on the top loss coefficient of FPSCs. Sol Energy 1991;2:83–7.
[9] Akhtar N, Mullick SC. Approximate method for computation of glass cover temperature and top heat-loss coefficient of solar collectors with single glazing. Sol Energy 1999;66:349–54.
[10] Akhtar N, Mullick SC. Computation of glass-cover temperatures and top heat loss coefficient of flat-plate solar collectors with double glazing. Energy 2007;32:1067–74.
[11] Smyth M, Eames PC, Norton B. Integrated collector storage solar water heaters. Renew Sust Energy Rev 2006;10:503–38.
[12] Kaldellis JK, Kavadias KA, Spyropoulos G. Investigating the real situation of Greek solar water heating market. Renew Sust Energy Rev 2005;9: 499–520.
[13] Batidzirai B, Lysen EH, van Egmond S, van Sark WGJHM. Potential for solar water heating in Zimbabwe. Renew Sust Energy Rev 2009;13:567–82.
[14] Muneer T, Asif M, Cizmecioglu Z, Ozturk HK. Prospects for solar water heating within Turkish textile industry. Renew Sust Energy Rev 2008; 12:807–23.
[15] Muneer T, Maubleu S, Asif M. Prospects of solar water heating for textile industry in Pakistan. Renew Sust Energy Rev 2006;10:1–23.
[16] Oliveira AC. A new look at the long-term performance of general solar thermal systems. Sol Energy 2007;81:1361–8.
[17] Bilgen E, Bakeka BJD. Solar collector systems to provide hot air in rural applications. Renew Energy 2008;33:1461–8.
[18] Koyuncu T. Performance of various designs of solar air heaters for crop drying applications. Renew Energy 2006;31:1073–88.
[19] Duffie JA, Beckmann WA. Solar Engineering of Thermal processes. New York: Wiley; 1980.
[20] Raja Sekhar Y, Sharma KV, Basaveswara Rao M. Evaluation of heat loss coefficients in solar flat plate collectors. ARPN Journal of Engineering and Applied Sciences 2009;4(5):15–9.
[21] Chaudhuri TK. Limitations of BIS design specifications for solar box cooker. J Sol Energy Soc India 1998;8:1–9.
[22] Farahat S, Sarhaddi F, Ajam H. Exergetic optimization of FPSCs. Renew Energy 2009;34:1169–74.
[23] El Fadar A, Mimet A, Perez-Garcıa M. Modelling and performance study of a continuous adsorption refrigeration system driven by parabolic trough solar collector. Sol Energy 2009;83:850–61.